Characterization of Oxides in Zirconium-based Alloys

A. Yilmazbayhan,[1] A. T. Motta,[1] R. J. Comstock,[2] B. Lai,[3] Z. Cai[3]
[1]Pennsylvania State University, University Park, PA, U.S.A.
[2]Westinghouse Electric Company, Pittsburgh, PA, U.S.A.
[3]Argonne National Laboratory, Argonne, IL, U.S.A.

Introduction

The corrosion kinetics of zirconium-based alloys in aqueous media are often described [1] in terms of two regimes: an initial pretransition region that is approximately parabolic with respect to time, followed by a region of more accelerated kinetics with an approximately linear dependence on time. The region of linear kinetic behavior is termed post-transition. The change from the parabolic to the linear regimes is called the transition, and it is described as either the exposure time or oxide thickness at which the change in kinetics occurs. However, a review of the corrosion data by using more scrutiny reveals that this simple description of the kinetics is only an approximation. The kinetics in pretransition are not parabolic but display a cubic dependence on time [2]. More importantly, the post-transition regime is composed of several periods of corrosion that mimic pretransition kinetics in a cyclical sequence. On individual samples, the cyclic nature of the kinetics can be easily distinguished through several repetitions. The cyclic nature of post-transition corrosion has been observed and noted for some time [3, 4], and observations [5-7] of stratification in the oxide films have been correlated with the cyclic kinetics.

This observation of the cyclic nature of corrosion is common among Zr alloys. Differences in the pretransition rate and oxide thickness at transition result in differences in corrosion resistance among the alloys. There is a great deal of empirical knowledge correlating alloy chemistry and microstructure to corrosion performance.

While such empirical knowledge is useful in optimizing the corrosion resistance of a particular alloy, there is little mechanistic understanding of how a given microstructure affects the cyclic nature (growth kinetics and thickness at transition) of the corrosion process.

Several independent pieces of evidence, including transmission electron micrography (TEM) and optical microscopy, show that there is periodicity in the oxides formed during autoclave exposures. Figure 1 shows optical micrographs (reflected light and transmitted light) of a cross-sectional sample from oxides formed on ZIRLO and Zircaloy-4 in 360°C water. A very regular repeating pattern is evident in the oxide, as revealed in the transmitted light pictures. Measurement of the fringe spacings reveals that they are extremely regular throughout the oxide and that different alloys exhibit different spacings. Figure 2 shows post-transition corrosion rates for the four alloys used in this study as a function of fringe spacing. The period length is in good agreement with the thickness of the oxide at transition, which is specific to the alloy. The post-transition corrosion rate varies inversely with the thickness of the oxide at transition.

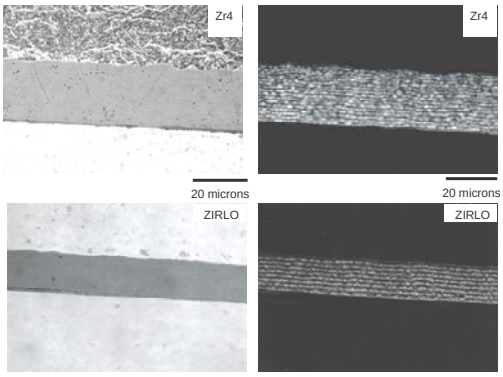

FIG. 1. Optical micrographs of oxides formed in ZIRLO and Zircaloy-4 in 360℃ pure water. (Left) reflected light; (right) transmitted light.

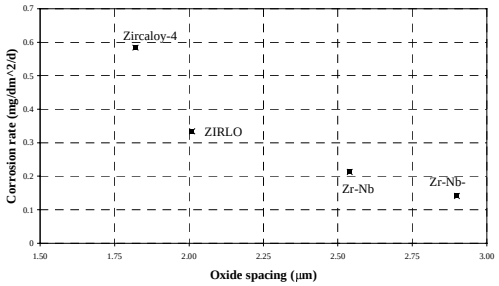

FIG. 2. Post-transition corrosion rates in pure water in four different alloys vs. oxide fringe spacing (or critical oxide thickness at transition).

Methods and Materials

In this study, the hypothesis was made that corrosion rate differences are related to the different oxide structures that are formed in different alloys. These different oxide structures cause the oxide to be a stronger

or weaker barrier to the transport of oxidizing species necessary for the corrosion front to advance. According to this hypothesis, if the differences in oxide structure were fully characterized, it would be possible to explain why different alloys have different corrosion rates. In this work, a systematic study was performed of the oxides formed on a series of Zr alloys (Zircaloy-4, ZIRLO, and Zr-Nb alloys), by using microfluorescence and microdiffraction techniques at the APS Synchrotron Radiation Instrumentation Collaborative Access Team (SRI-CAT) beamline 2-ID-D. Oxides that formed on commercial alloys in water, steam, and lithiated water environments and exhibited a range of different corrosion rates were examined. The goal was to identify the most significant differences in oxide microstructure that could be related to the differences in observed alloy corrosion behavior.

All alloys in water follow approximately the same pretransition kinetics, which means that the same transport mechanism and the same transport rates are applicable. However, all these alloys undergo oxide transition at different times, indicating that they have a different critical oxide thickness for transition. Since the rate of oxide growth in the latter part of the pretransition regions is low, it follows that a small change in the critical thickness for transition results in large changes in the post-transition corrosion rate.

In this study, a unique x-ray probe developed at the SRI-CAT sector that can focus the synchrotron beam down to a 0.25×0.3-μm spot on the sample was used. This allows diffraction and fluorescence information to be obtained in a spatially resolved manner with much greater precision than previously achievable. In these experiments, cross-sectional oxide samples were examined by performing detailed scans (0.15-μm steps) of oxides that ranged in thickness from 5 to 33 μm. At each location, a diffraction pattern and a fluorescence profile were acquired. Diffraction patterns were recorded with a charge-coupled device (CCD) with an imaging area of 6.78×6.28 cm and a 1241×1151-pixel resolution.

To get 1-D diffraction patterns, each diffraction image was integrated by using a computer program. Then the diffraction peaks in the pattern were fitted to a function by using the Peak Fit computer program to find the peak positions and the integrated intensity of each peak. By using the Garvie formula [8], the tetragonal oxide to monoclinic oxide (T/M) ratio was calculated. Grain sizes in the oxide were calculated by using line broadening of the diffraction peaks.

Results

From the fluorescence data, no large-scale redistribution of alloying elements was observed in the alloys studied. In particular, no significant changes were seen in the levels of Sn from the metal to the oxide in any of the alloys. A peak of Fe was normally observed on the outer part of the oxides; it was due to pickup of dissolved Fe in the autoclave water. This autoclave contamination also helped reveal the unique features of the oxide structure. The contamination is revealed in detail in this work because of the unique combination of spatial and elemental sensitivity in x-ray microfluorescence (at the parts-per-million [ppm] level), and it is identified because of the joint presence of Fe and Mn. Figure 3 shows a fluorescence scan across the oxide thickness in ZIRLO oxide formed in lithiated water. The levels of Fe observed in oxides formed in lithiated water are considerably higher than those found in oxides formed in water or steam, suggesting that the oxides formed in lithiated water are more porous. The periodicity in the microfluorescence observed in these oxides is also in good agreement with the observed transition thicknesses and with the fringe spacing shown in Fig. 1.

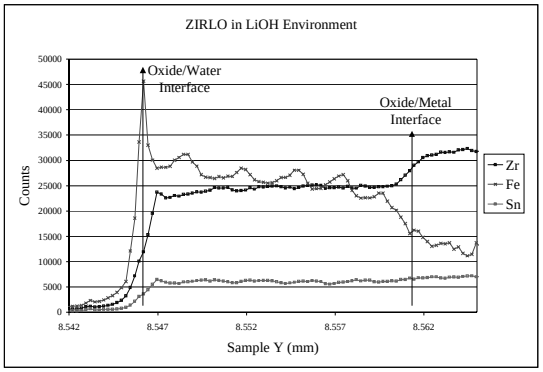

FIG. 3. Microfluorescence scans obtained by using synchrotron radiation for oxide formed in ZIRLO tested in lithiated water, as a function of distance along the oxide.

For the diffraction studies, the high number of photons and the low background, combined with the spatial resolution of the microprobe, mean that very small volume fractions of second phases can be detected and that details about the phases, such as grain size and their detailed texture, can be obtained at the submicrometer scale. This allowed, for the first time, direct measurements of the variation of the tetragonal-phase fraction with distance from the oxide-metal interface. One such measurement, showing the tetragonal-fraction variation along an oxide formed in ZIRLO in water, is shown in Fig. 4.

The region closest to the oxide-metal interface was identified in this work with higher T/M ratios. From x-ray line broadening, the monoclinic grain size increases with distance from the oxide-metal interface, while the tetragonal phase exhibits an approximately constant grain size that is shown in Fig. 5. The monoclinic-phase texture

also evolves within the first 2 or 3 μm, becoming more isotropic with increasing distance from the interface. In the oxides with the most protective barrier layers, mostly columnar grains are observed right up to the oxide-metal interface.

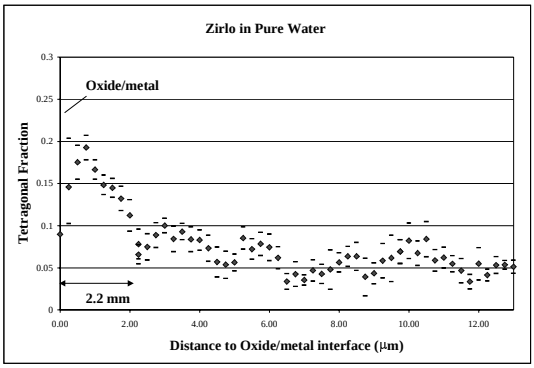

FIG. 4. Tetragonal fraction in oxide formed in ZIRLO tested in 360℃ pure water, calculated from synchrotron radiation micro-x-ray diffraction, vs. distance from the oxide-metal interface.

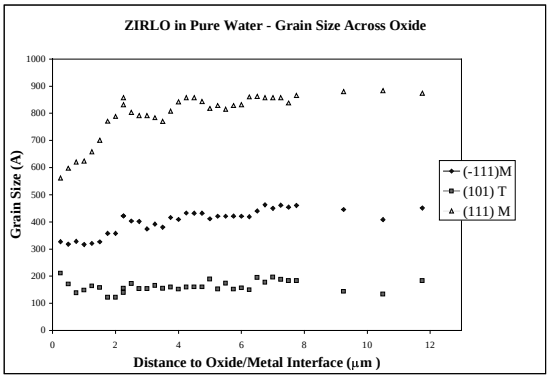

FIG. 5. Grain size as calculated from the three peaks involved in the calculation of the tetragonal-phase fraction across the oxide of ZIRLO in pure water.

Discussion

The oxides formed in 360°C water containing 70 ppm of LiOH are qualitatively different from those formed in either water or steam. Unlike the samples tested in pure water, periodicity in the oxide is only observed in ZIRLO, not in Zircaloy-4 or Zr-Nb. This retention of the periodicity in ZIRLO correlates with the good corrosion resistance of this alloy in lithiated water. Thus, the observed optical periodicity can be seen as an indication of a more orderly formation of protective oxide, which is further evidence that the periodicity observed is a good indicator of corrosion behavior. This is confirmed by microfluorescence measurements that show much higher ingress of elements from the autoclave during a lithiated water test in Zr-Nb oxide than in ZIRLO.

The studies demonstrated the ability to identify the phases present (monoclinic and tetragonal or cubic zirconia, zirconium hyrides, and zirconium metal) and resolve them spatially in the oxide. It was found that the tetragonal fraction ranges from 0% to about 15% and that the first 2 and 3 μm near the oxide-metal interface are richer in the tetragonal phase than is the remainder of the oxide by a factor of 2 or 3. This tetragonal-rich region is within the protective nontransitioned oxide layer. In Fig. 4, a periodicity in the tetragonal fraction that corresponds well with the evidence of periodicity in the oxide seen by other techniques was detected.

In comparing the fraction of the tetragonal oxide in the protective layer of the different alloys, it was found that oxides formed in water and steam on Zircaloy-4 and ZIRLO had similar fractions, but that Zr-Nb had lower amounts. However, the fraction was much smaller, indicating a degradation of the protective layer in the presence of LiOH.

Acknowledgments

This research has been supported by the U.S. Department of Energy (DOE) Nuclear Energy Research Initiatives (NERI) Program. The use of the APS was supported by the DOE Office of Science, Office of Basic Energy Sciences, under Contract No. W-31-109-ENG-38. We wish to thank the SRI-CAT personnel.

References

[1] D. E. Thomas, *Metallurgy of Zirconium,* edited by B. Lustman and F. Kerze (McGraw-Hill Book Co., New York, NY, 1955), p. 608.

[2] G. P. Sabol and S. B. Dalgaard, J. Electrochem. Soc. **122**, 316 (1975).

[3] B. Griggs, H. P. Maffei, and D. W. Shannon, J. Electrochem. Soc. **109**, 665(1962).

[4] A. Kiselev, V. A. Myshkin, A. V. Kozhevnikov, S. I. Korolev, and E. G. Shorina, Cor. of React. Mater. **2**, 67 (1962).

[5] B. Cox, J. Nucl. Mater. **29**, 50 (1969).

[6] G. P. Sabol, S. G. McDonald, and G. P. Airey, *Microstructure of the Oxide Films formed on Zirconium-based Alloys,* STP 551 (ASTM, 1974), p. 435.

[7] G. P. Sabol and S. G. McDonald, *Stress Effects on the Oxidation of Metals* (AIME, 1975), p. 352.

[8] R. C. Garvie, P. J. Nickolson, J. Am. Ceram. Soc. **57**, 22 (1974).